Determination of NTA and EDTA and Speciation of Their Metal Complexes in Aqueous Solution by Capillary Electrophoresis

ARTICLE *in* ENVIRONMENTAL SCIENCE AND TECHNOLOGY · JANUARY 2000

Impact Factor: 5.33 · DOI: 10.1021/es990309m

6 AUTHORS, INCLUDING:

Gary Owens
University of South Australia
73 PUBLICATIONS **1,576** CITATIONS
SEE PROFILE

Ian Singleton
Edinburgh Napier University
60 PUBLICATIONS **1,721** CITATIONS
SEE PROFILE

Frank Andrew Smith
University of Adelaide
229 PUBLICATIONS **11,768** CITATIONS
SEE PROFILE

Environ. Sci. Technol. **2000**, *34,* 885−891

Determination of NTA and EDTA and Speciation of Their Metal Complexes in Aqueous Solution by Capillary Electrophoresis

GARY OWENS,*,† VERITY K. FERGUSON,† MICHAEL J. MCLAUGHLIN,†,‡ IAN SINGLETON,† ROB J. REID,§ AND F. A. SMITH||

Department of Soil and Water and Department of Plant Science, Waite Campus, University of Adelaide, Glen Osmond, South Australia 5064, Australia, CSIRO Land and Water, PMB No. 2, Glen Osmond, South Australia 5064, Australia, Department of Environmental Biology, University of Adelaide, South Australia 5005, Australia

The interest in the use of chelates for enhancing metal uptake by plants during phytoremediation and their widespread use in plant nutrient research requires that an easy, reproducible method be developed for chelate detection in a variety of systems. This work examined the use of capillary electrophoresis for chelate analysis. Electropherograms for nitrilotriacetic acid (NTA) and ethylenediaminetetraacetic acid (EDTA) and their metal complexes were obtained by capillary electrophoresis in a phosphate buffer by direct UV detection at 185 nm. The metals used were Ca(II), Co(II), Ni(II), Cu(II), Zn(II), Cd(II), Pb(II), and Fe(III). For the majority of metals studied, linear calibration curves were obtained in the concentration range of 10−1000 μM. The direct method of determination at 185 nm was found to give a higher detection sensitivity than direct detection at 254 nm. Limits of detection for the metal chelate complexes were in the range of 2−50 μM. The analysis was fast (<6 min), exhibited low relative standard deviations for retention time (<1%) and peak corrected area (<5%), and required no complex sample pretreatment. The method was used to demonstrate speciation in complex nutrient media.

Introduction

Ethylenediaminetetraacetic acid (EDTA) and nitrilotriacetic acid (NTA) are two aminocarboxylic acids known to increase metal uptake by plants (*1*−*3*). It is generally believed that, in conjunction with the use of either suitable hyperaccumulator species or high biomass crops, the addition of chelates to contaminated soils may assist in the phytoremediation process. However, the stability of EDTA and NTA under environmental conditions is not known with any certainty. Knowledge of the environmental fate of these compounds when used as soil amendments is considered vital because of their ability to mobilize heavy metals. In addition, studies of metal uptake by plants in nutrient solution culture often rely on the use of chelates such as NTA or EDTA to buffer free metal ion activities to low levels simulating environmental media (*4*). Knowledge of the stability of metal-chelate complexes and free chelate ions in nutrient solutions is lacking due to the difficulty of analysis. Therefore, to study the degradation of these chelates there is a need to develop methods capable of analyzing small sample volumes at environmental concentrations with relatively short sampling times. Capillary electrophoresis (CE) is one such method that fulfills all these criteria.

Traditional methods for the determination of EDTA include HPLC (*5*), GC (*6*), or IC (*7*) and usually rely on the derivatization of the free chelate to a UV-absorbing metal complex prior to analysis. Methods for the detection of chelates or their associated metal complexes have also been reported in a variety of background matrixes including biological fluids (*8*), environmental waters (*9*), and foodstuffs (*10*). Many of these methods are not generally applicable to a wide variety of conditions and do not specifically determine both chelate and metal-chelate moieties simultaneously. In addition, these methods often require complex pretreatment of the samples prior to analysis. Even when free EDTA is detected, it is usually of much lower absorbance than the corresponding chelate complex and has a broad distorted peak of little analytical value (*11*).

Baron and Hering (*12*) recently reported the simultaneous analysis of uncomplexed EDTA and various metal-EDTA complexes by electrospray mass spectrometry (ES/MS) with detection limits of about 1 μM. This is a promising tool for speciation studies concerning the environmental fate of organic chelates. However, ES/MS is beyond the scope of many analytical laboratories and has yet to be accepted as a routine method of analysis. CE seems to be a simpler and less expensive instrumental alternative.

Recent papers have concentrated on using direct detection of UV-absorbing metal-chelate complexes formed either on column (*11*, *13*−*16*) or prior to CE analysis off column (*9*, *17*−*19*) to determine trace amounts of metal in the sample. These studies consistently use wavelengths ≥200 nm. This probably results from the usual practice of indirect determination at these higher wavelengths as a default method for many commercial machines. Recently Bürgisser and Stone (*20*) reported a method for the determination of a variety of amino carboxylic acids at 185 nm that had the ability to simultaneously determine the chelate-metal complex and thus allow speciation to be readily studied. Bürgisser and Stone's work dealt solely with Co. In this work CE was used to examine the speciation of EDTA and NTA with a large range of metals.

Experimental Section

Materials. Water was obtained from a Milli-Q purification system and had a resistance greater than 18 MΩ·cm. All chemicals used were analytical grade reagents. Tetradecyl trimethylammonium bromide (TTAB) was obtained from Aldrich and was used without purification. Nitrilotriacetic acid (NTA) was obtained from Sigma, and ethylenediaminetetraacetic acid disodium salt dihydrate (Na_2EDTA) was obtained from Merck. 4-Morpholineethanesulfonic acid (MES) was obtained from BDH, and *N*,*N*′-di(2-hydroxylbenzyl)ethylenediamine *N*,*N*′-diacetic acid dihydrochloride dihydrate (HBED) was from Strem Chemicals. IR-120 cation-exchange resin (H form) was purchased from Sigma and conditioned prior to use. The resin was soaked in 1 M nitric

* Corresponding author tel: 61 8 8303 6587; fax: 61 8 8303 8565; e-mail: gowens@waite.adelaide.edu.au.
† Department of Soil and Water, University of Adelaide.
‡ CSIRO Land and Water.
§ Department of Plant Science, University of Adelaide.
|| Department of Environmental Biology, University of Adelaide.

10.1021/es990309m CCC: $19.00
Published on Web 01/21/2000

acid overnight and rinsed with water until the influent pH and effluent pH were identical.

Solutions. All dilutions were typically made by weight from 5 or 2 mM stock solutions. Metal stock solutions were prepared from analytical grade chloride, nitrate, or sulfate salts. Metal complex solutions were prepared by direct mixing of a portion of the appropriate metal stock solution with the amino carboxylic acid stock solution in the mole ratio of 1:1, 1:2, or 2:1. All aqueous metal complex solutions were allowed to stand overnight to ensure that a thermodynamic equilibrium was established prior to analysis by CE.

Full nutrient solution contained 1.2 mM KNO_3, 1.45 mM $MgSO_4 \cdot 7H_2O$, 25 μM FeHBED, 2 mM MES, 10 μM $MnCl_2 \cdot 4H_2O$, 3.55 mM $Ca(NO_3)_2 \cdot 4H_2O$, 10 μM NaCl, 75 μM KH_2PO_4, 30 μM H_3BO_3, 0.2 μM $Na_2MoO_4 \cdot 4H_2O$, 0.2 μM $CuCl_2$, 10 nM $CdCl_2$, and 1 μM $ZnSO_4 \cdot 7H_2O$ (*21*). The final pH of this solution was adjusted to 6.1 by the addition of NaOH.

Capillary Electrophoresis. Electropherograms were obtained on a capillary ion analyzer (CIA Millipore Waters) using a negative power supply with a 75 μm i.d. fused silica capillary of 60 cm total length (52.5 cm to the detector). The carrier electrolyte was 25 mM phosphate buffer ($Na_2HPO_4 \cdot 2H_2O/KH_2PO_4$) (*22*), equivalent to 50 mM phosphate, and 0.5 mM TTAB (pH 6.86). The addition of TTAB reverses the direction of electrophoretic flow (*23*) so that there is a net flow toward the detector and results in shorter migration times for the anions and better peak shapes. The addition of a surfactant, such as TTAB, has the added advantage of occupying reactive silanol sites within the capillary that may otherwise be occupied by metal ions or the free aminocarboxylic acids under investigation (*24*).

Samples were injected in the hydrostatic mode for 30 s at 10 cm. The operating conditions for a run typically included 20 kV generated by the negative power supply after equilibration to 25 °C. Between each run the capillary was purged with phosphate buffer for 2 min. At the end and start of each day, the capillary was conditioned by sequentially purging with 0.1 M NaOH (5 min), 0.01 M NaOH (5 min), and MilliQ water for at least 20 min. Prior to commencement of runs for the day, the capillary was additionally purged with buffer for at least 20 min. All solutions were filtered through 0.45 μM disposable filters prior to analysis. A few solutions were additionally degassed using ultrasonication, but this seemed to have no noticeable effect on the electropherograms.

Direct UV detection at either 185 or 254 nm was used. The wavelengths of analysis were changed using the appropriate filters and lamp covers supplied with the machine. The absorbance was converted to millivolts using a SATIN A/D converter (1 AU = 1 V) interfaced with a 200 MHz Pentium computer. Electropherograms were processed using commercial Millenium software.

Unknown peaks were unequivocally identified by spiking with known solutions. Quantification was accomplished using peak area divided by retention time rather than peak area alone. This allowed for any variation of run times due to the condition of the capillary and gave better reproducibility than area alone. The detection limit was defined as the concentration at which the signal-to-baseline noise ratio, (S/N) equaled 3. Detection limits were determined from log−log plots of S/N versus concentration in the range of 10−1000 μM or by interpolation of specifically prepared low-concentration solutions in the range of 2−50 μM. Generally log−log plots were found to eliminate slight curvature present in linear plots of S/N with concentration and therefore resulted in a better relationship. Reproducibilities of 1% and 5% in retention time and peak area, respectively, were considered acceptable.

Results and Discussion

GEOCHEM Speciation Calculations. Bürgisser and Stone (*20*) highlighted the possibility of altered analyte speciation due to chemical reaction with the carrier electrolyte once the sample was injected for CE analysis. For this reason, speciation calculations were performed using GEOCHEM (*25*) under conditions expected to occur in the carrier electrolyte (50 mM PO_4^{3-}, 50 mM Na^+, 25 mM K^+, 1 mM CO_3^{2-}, and pH 6.86). The results from these calculations are summarized in Tables 1−2 along with protonation level and molecular charge.

Speciation calculations for EDTA indicate that in the absence of metal at pH 6.86 the concentration of $[EDTA]^{4-}$ is extremely small. The dominant species are $[HEDTA]^{3-}$ (83%) and $[H_2EDTA]^{2-}$ (17%). These values are similar to the speciation previously calculated using HYDRAQL (*20*). In the presence of metal ions, the dissociation equilibrium is shifted to the formation of $[EDTA]^{4-}$ by complex formation, and the dominant species is $[MEDTA]^{2-}$, which is present in nearly 100% for all the metals studied.

In the absence of any metal, the speciation calculations indicated that NTA exists exclusively as $[HNTA]^{2-}$ (100%). In the presence of metal, the predominant species remains a 1:1 complex $[MNTA]^{2-}$, present in lower percentages than the corresponding EDTA complexes. This is to be expected based on the lower formation constants of NTA. GEOCHEM calculations predicted the formation of significant metal precipitates with the phosphate buffer for Cd, Pb, and Fe(III) when NTA was the ligand. This would seem to not solely be a function of formation constants as Pb and Zn have similar log K values (12.7 and 12.0) but were predicted to have hugely different speciations (25.6% and 96.8%). GEOCHEM predicted that any metal not complexed by chelate would be present almost entirely as a solid formed by reaction with phosphate in the buffer. However, during experiments no obvious precipitates were formed, and no fouling of the capillary occurred in any of the runs. It may be that the short run times were insufficient to allow precipitation to occur or that any precipitates were unstable under the conditions employed in CE analysis. Therefore, GEOCHEM calculations were repeated specifically precluding the possibility of metal precipitates with the buffer. There was a resulting increase in predicted concentrations of the metal NTA species for all of the metals studied (Table 2).

Detection of Free and Complexed Aminocarboxylic Acids. Initial CE experiments conducted at 254 nm indicated that the metal complexes of Co(II), Cu(II), Pb(II), and Fe(III) could be detected with both EDTA and NTA. However, the free metal chelates were not generally detected at analytically useful levels, and the absorbance of the complexes was also low. No complexes of Ni(II) or Zn(II) could be detected with either ligand at this wavelength. At 185 nm the absorption of all species increased, so that all of the above metals were detected as complexes in addition to the free carboxylic acid. For this reason, 185 nm was chosen for all subsequent experiments.

In CE analysis, the main factors affecting the separation are applied voltage, pH, and buffer composition. At voltages below 20 kV, peak resolution was poor while higher voltages resulted in an error condition on the machine most likely due to bubble formation around electrodes due to excessive heating. A higher pH was not considered, as speciation would become more complicated due to increased hydrolysis of metal ions. Runs using 10 mM phosphate buffer and 0.5 mM TTAB also resulted in a poor peak shape.

Common anions such as chloride and nitrate did not interfere directly with the detection of the amino carboxylic acids studied here or with their metal complexes, since their

TABLE 1. Speciation of Metal-Chelate Complexes Formed with EDTA (L^{4-}) under Conditions Experienced during CE Analysis

metal	equation	log K[a]	complex	speciation[b] (%)	detection limit[c] (μM)
Co(II)	ML/M·L	18.2	$[Co(II)L]^{2-}$	100	2
	MHL/M·H·L	21.6	$[Co(II)HL]^{-}$	0	
	$MH_2L/M·H^2·L$	24.1	$[Co(II)H_2L]^{0}$	0	
Ni(II)	ML/M·L	20.1	$[Ni(II)L]^{2-}$	100	2
	MHL/M·H·L	23.7	$[Ni(II)HL]^{-}$	0	
	$MH_2L/M·H^2·L$	25.2	$[Ni(II)H_2L]^{0}$	0	
	M(OH)L/M·OH·L	7.6	$[Ni(II)(OH)L]^{3-}$	0	
Cu(II)	ML/M·L	20.5	$[Cu(II)L]^{2-}$	100	7
	MHL/M·H·L	24.0	$[Cu(II)HL]^{-}$	0	
	$MH_2L/M·H^2·L$	26.3	$[Cu(II)H_2L]^{0}$	0	
	M(OH)L/M·OH·L	8.5	$[Cu(II)(OH)L]^{3-}$	0	
Zn(II)	ML/M·L	18.2	$[Zn(II)L]^{2-}$	100	3
	MHL/M·H·L	21.7	$[Zn(II)HL]^{-}$	0	
	$MH_2L/M·H^2·L$	23.3	$[Zn(II)H_2L]^{0}$	0	
	M(OH)L/M·OH·L	6.0	$[Zn(II)(OH)L]^{3-}$	0	
Cd(II)	ML/M·L	18.2	$[Cd(II)L]^{2-}$	100	6
	MHL/M·H·L	21.6	$[Cd(II)HL]^{-}$	0	
	$MH_2L/M·H^2·L$	23.6	$[Cd(II)H_2L]^{0}$	0	
	M(OH)L/M·OH·L	4.1	$[Cd(II)(OH)L]^{3-}$	0	
Pb(II)	ML/M·L	19.7	$[Pb(II)L]^{2-}$	100	2
	MHL/M·H·L	23.0	$[Pb(II)HL]^{-}$	0	
Ca(II)	ML/M·L	12.4	$[Ca(II)L]^{2-}$	97.8	510
	MHL/M·H·L	15.9	$[Ca(II)HL]^{-}$	0.2	
Fe(III)	ML/M·L	27.7	$[Fe(III)L]^{-}$	80.4	12
	MHL/M·H·L	29.2	$[Fe(III)HL]^{0}$	0	
	M(OH)L/M·OH·L	19.9	$[Fe(III)(OH)L]^{2-}$	19.4	
	$M_2(OH)_2L_2/M^2·OH^2·L^2$	40.4	$[Fe(III)_2(OH)_2L_2]^{4-}$	<0.1	

[a] Thermodynamic stability constant (K) corrected to zero ionic strength [from GEOCHEM database (*25*)]. [b] Speciation was calculated using GEOCHEM for 500 μM ligand and metal under CE analysis conditions (50 mM PO_4^{3-}, 50 mM Na^+, 25 mM K^+, 1 mM CO_3^{2-}, pH 6.86). [c] Detection limits of metal complexes were determined at 185 nm under CE analysis conditions when S/N = 3.

TABLE 2. Speciation of Metal-Chelate Complexes Formed with EDTA (L^{4-}) under Conditions Experienced during CE Analysis

metal	equation	log K[a]	complex	speciation[b] (%)	detection limit[c] (μM)
Co(II)	ML/M·L	11.0	$[Co(II)L]^{-}$	98.0	440
	$ML_2/M·L^2$	12.0	$[Co(II)L_2]^{4-}$	0	
	M(OH)L/M·OH·L	0.4	$[Co(II)(OH)L]^{2-}$	0	
Ni(II)	ML/M·L	12.8	$[Ni(II)L]^{-}$	99.4	7
	$ML_2/M·L^2$	17.0	$[Ni(II)L_2]^{4-}$	0	
	M(OH)L/M·OH·L	1.5	$[Ni(II)(OH)L]^{2-}$	0	
Cu(II)	ML/M·L	14.4	$[Cu(II)L]^{-}$	99.2	30
	MHL/M·H·L	16.2	$[Cu(II)HL]^{0}$	0	
	$ML_2/M·L^2$	18.2	$[Cu(II)L_2]^{4-}$	0	
	M(OH)L/M·OH·L	4.8	$[Cu(II)(OH)L]^{2-}$	0.4	
Zn(II)	ML/M·L	12.0	$[Zn(II)L]^{-}$	98.2[d]	13
	$ML_2/M·L^2$	14.9	$[Zn(II)L_2]^{4-}$	0	
	M(OH)L/M·H·L	1.5	$[Zn(II)(OH)L]^{2-}$	0.1	
Cd(II)	ML/M·L	11.1	$[Cd(II)L]^{-}$	97.8[d]	
	$ML_2/M·L^2$	15.0	$[Cd(II)L_2]^{4-}$	2.1	
	M(OH)L/M·OH·L	−0.6	$[Cd(II)(OH)L]^{2-}$	0	
Pb(II)	ML/M·L	12.7	$[Pb(II)L]^{-}$	100[d]	
Ca(II)	ML/M·L	7.7	$[Ca(II)L]^{-}$	27.2[d]	
	$ML_2/M·L^2$	9.5	$[Ca(II)L_2]^{4-}$	<0.1	
Fe(III)	ML/M·L	17.9	$[Fe(III)L]^{0}$	0.2[d]	
	$ML_2/M·L^2$	26.2	$[Fe(III)L_2]^{3-}$	0.2	
	M(OH)L/M·OH·L	13.5	$[Fe(III)(OH)L]^{-}$	90.0	
	$M(OH)_2L/M·OH^2·L$	5.3	$[Fe(III)(OH)L]^{2-}$	8.6	

[a] Thermodynamic stability constant (K) corrected to zero ionic strength [from GEOCHEM database (*25*)]. [b] Speciation was calculated using GEOCHEM for 500 μM ligand and metal under CE analysis conditions (50 mM PO_4^{3-}, 50 mM Na^+, 25 mM K^+, 1 mM CO_3^{2-}, pH 6.86). [c] Detection limits of metal complexes were determined at 185 nm under CE analysis conditions when S/N = 3. [d] Calculations assume no metal precipitate with buffer.

charge density is much larger and these anions therefore eluted more rapidly (typically in less than 2 min). Sulfate did not absorb (significantly) at 185 nm.

Reproducibilities were determined from 10 successive injections. As an illustration of the high reproducibility obtainable, for 500 μM EDTA in water, the relative standard deviations for retention time and peak corrected area were 0.36% and 0.99% respectively.

At 185 nm the detection limit for EDTA was 50 μM, slightly higher than for NTA (10 μM). The higher value for EDTA has been observed previously and was attributed to baseline rising and peak broadening of EDTA due to greater adsorption to the capillary wall by EDTA when compared to NTA (*20*).

The detection limits for the metal complexes appearing in Tables 1 and 2 were generally good and ranged from 2 to 50 μM with two exceptions. CoNTA and CaEDTA had

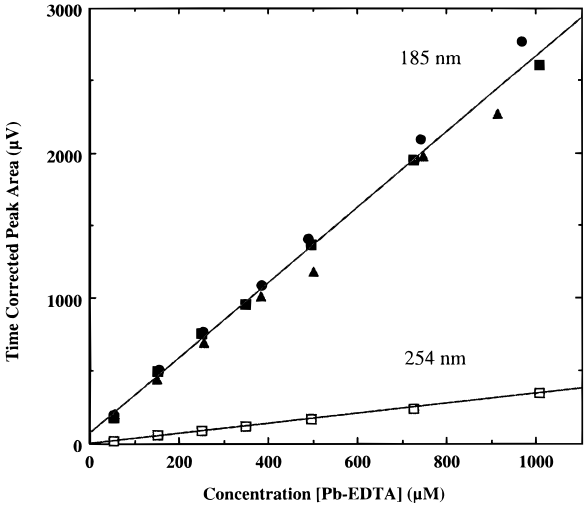

FIGURE 1. Effect of wavelength and mole ratio on the calibration curves of PbEDTA. The mole ratio of metal to ligand was as follows: squares, 1:1; circles, 1:2; triangles, 2:1. Filled symbols, 185 nm; open symbols, 254 nm. Solid curves represent lines of best fit obtained by simple linear regression.

unusually high limits of detection when compared to all other complexes. The high detection limit of CoNTA has been observed previously and attributed to ligand exchange in the buffer prior to the complex reaching the detector (*20*). We also found a much higher detection limit (440 μM) than that approximated by Bürgisser and Stone ($\approx$100 μM). The higher detection limit found here is due to the higher effective buffer concentration used. A higher phosphate concentration would favor ligand exchange and result in the observed higher limit of detection.

Even at low concentrations, the presence of CaEDTA caused a rise in the baseline, and no distinct peak attributable to CaEDTA could be detected below 500 μM. Electropherograms of 500 μM EDTA in water containing increasing concentrations of Ca showed that as the concentration of Ca increased there was a corresponding decrease in the free EDTA peak, indicative of complex formation, but there was no corresponding evolution of a CaEDTA peak. Removal of Ca by passing solutions through a cation-exchange resin, Amberlite IR-120 in the hydrogen form, and rerunning the electropherograms showed substantial regeneration of the free EDTA peak. These results indicated that CaEDTA formed to some extent but had an extremely high detection limit in the phosphate buffer. This may be due to incomplete complex formation prior to analysis or due to an instability of the complex during the CE analysis.

Calibration curves obtained for the PbEDTA complex at 185 nm corresponding to the molar ratios of Pb to EDTA of 1:1, 1:2, and 2:1 are superimposed in Figure 1 together with the calibration curve for the 1:1 PbEDTA complex determined at 254 nm. The line of best fit is for the three combined sets of data and had a slope with a standard deviation that covered the individual standard deviations of all three curves. There was therefore no significant difference between the three curves, indicating that a slight excess of either metal or chelate did not adversely affect the equilibrium of chelate formation. Similar curves were obtained for CuEDTA and CoEDTA. In comparison, the calibration curve for the identical 1:1 complex of PbEDTA determined at 254 nm had a much smaller slope, indicative of a much lower absorbance by this complex at the higher wavelength.

At low concentrations, metal-EDTA complex peaks were broad and perturbed, but this did not affect the linearity of the calibration curves. All calibration curves had regression coefficients approaching unity. The broadness of these peaks

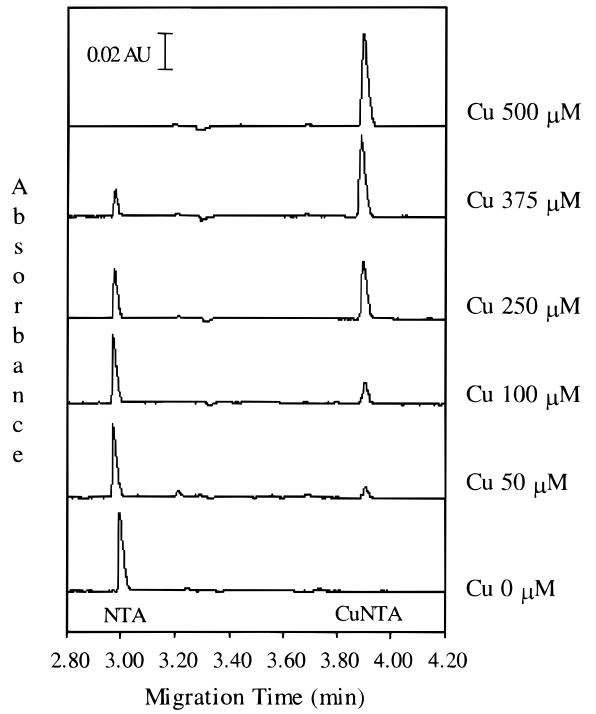

FIGURE 2. Stacked electropherograms for aqueous solutions of 500 μM NTA containing increasing proportions of copper. Conditions: 25 mM phosphate buffer and 0.5 mM TTAB (pH 6.86), 185 nm, 20 kV, 25 °C. AU = absorbance units.

may be due to adsorption of the complex on to the capillary wall as discussed above.

Speciation by CE Analysis. Five stacked electropherograms for a 500 μM NTA solution containing increasing amounts of $CuSO_4$ are shown in Figure 2. In the absence of any copper, only a single peak occurs at 2.97 min corresponding to free NTA. With increasing amounts of copper, a peak near 3.90 min appears corresponding to the CuNTA complex. When the amount of copper is present in equimolar concentrations with NTA, only a single peak corresponding to the CuNTA complex is observed. When the metal complex was detected, such speciation plots were observed for all metals considered in this paper with both NTA and EDTA.

Separate calibration curves for chelate and chelate complex in the concentration range of 10−1000 μM were prepared and used to determine the concentration of individual species in a mixed sample. The concentrations of each species obtained using the CE technique was compared with the concentrations predicted using GEOCHEM under conditions expected to occur in the phosphate buffer. The concentration of ligand was fixed at 500 μM, and the metal concentration varied from 0 to 500 μM. A typical plot of CE-derived concentrations against predicted GEOCHEM concentrations is shown in Figure 3. There was good agreement between the experimental and predicted concentrations confirming the utility of the CE technique.

Mobilities. The effective mobility of a species m, undergoing electroosmotic migration is given by

$$\mu_m = \frac{L_t L_d}{V}\left(\frac{1}{t_m} - \frac{1}{t_{eo}}\right) \quad (1)$$

where L_t and L_d are respectively the total capillary length and length to detector in cm, t_m is the retention time for the moiety under consideration, t_{eo} is the retention time for the electrolyte solution, and V is the voltage applied across the capillary. t_{eo} may be determined as the time a neutral species takes to pass through the capillary.

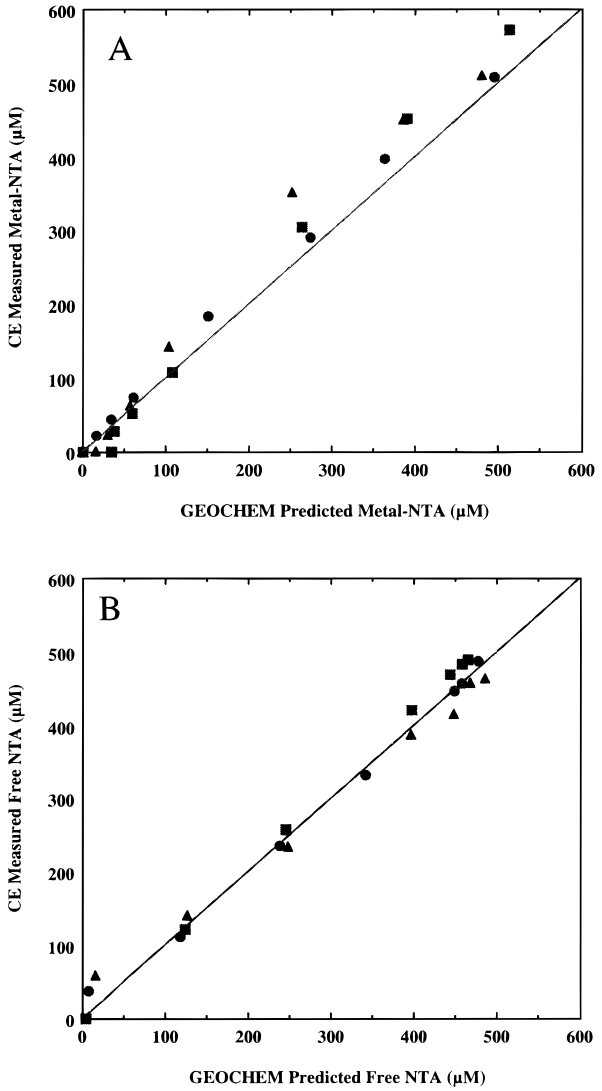

FIGURE 3. Correlation between experimentally determined CE concentrations and predicted GEOCHEM concentrations for metal-NTA (A) and NTA (B) in an aqueous solution of 500 μM NTA containing different amounts of metal. Squares, Cu; circles, Ni; triangles, Zn. The solid line shows the theoretical 1:1 relationship between the two concentrations.

The electroosmotic flow time t_{eo} was taken to be the elution time of a large negative water peak that eluted near 6 min. Spiking of the solution with methanol resulted in a positive peak with an elution time identical to the water peak and confirmed the utility of the water peak as a marker for electroosmotic flow. Initially the mobility of the chloride anion was determined in the concentration range of 10−1000 μM. The average mobility determined using eq 1 was $(8.00 \pm 0.04) \times 10^{-4}$ cm^2 V^{-1} s^{-1}, which agreed well with the literature value of 7.91 cm^2 V^{-1} s^{-1} (*26*). In the same concentration range, the average mobilities of the aminocarboxylic acids were $(5.24 \pm 0.05) \times 10^{-4}$ cm^2 V^{-1} s^{-1} for NTA and $(5.11 \pm 0.11) \times 10^{-4}$ cm^2 V^{-1} s^{-1} for EDTA. This supported the observation that, in an equimolar mixture of both ligands, NTA has a higher mobility and eluted slightly before the larger and slower moving EDTA moiety, despite it having a greater charge.

The average mobilities of each metal-chelate complex were also determined using eq 1. The mobilities of the metal-EDTA complexes shown in Table 3 agreed well with those determined by Padarauskas and Schwedt (*23*) in a 10 mM phosphate buffer at pH 8. As the ionic strength of the buffer is increased, the effective mobility is expected to decrease (*23*). Thus at the higher ionic strength used here the observed effective mobilities should be consistently lower than those determined by Padarauskas and Schwedt. This is true for all the complexes studied in Table 3 with the exception of Fe(III)EDTA, which has a slightly higher mobility at higher ionic strength. The difference is probably within experimental error. The slight discrepancy cannot be attributed to increased formation of $[Fe(III)(OH)EDTA]^{2-}$ at pH 8, since this would tend to increase the effective mobility.

TABLE 3. Average Effective Mobilities for Metal Chelates in the Concentration Range 10−1000 μM[a]

	μ_m (10^4 cm^2 V^{-1} s^{-1})		
metal	NTA	EDTA	EDTA[b]
Co(II)	2.87 ± 0.02[c]	4.37 ± 0.07	4.62
Ni(II)	2.71 ± 0.04	4.27 ± 0.09	4.58
Cu(II)	3.17 ± 0.05	4.56 ± 0.12	4.61
Zn(II)	3.03 ± 0.03	4.30 ± 0.09	
Cd(II)	*d*	4.01 ± 0.04	
Pb(II)	*d*	4.41 ± 0.09	4.55
Fe(III)		3.80 ± 0.05[e]	3.71

[a] Conditions: electrolyte 25 mM phosphate buffer, pH 6.86, 20 kV. The error refers to one standard deviation of the mean. [b] Ref *23*. [c] Average of four values due to higher limit of detection of this species. [d] No apparent peak. [e] Average of two runs.

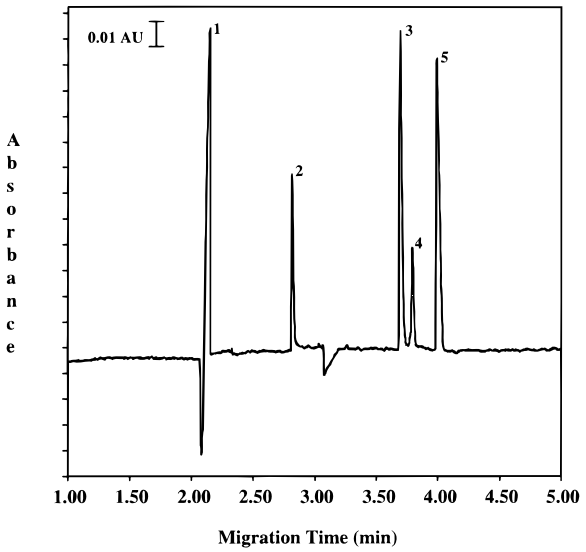

FIGURE 4. Electropherogram of an aqueous solution containing 2 mM NTA, 0.5 mM $CuSO_4$, 0.5 mM $NiCl_2$, and 0.5 mM $ZnCl_2$. Peak identity: (1) Cl; (2) NTA; (3) CuNTA; (4) ZnNTA; (5) NiNTA. Conditions: 25 mM phosphate buffer and 0.5 mM TTAB (pH 6.86), 185 nm, 20 kV, 25 °C. AU = absorbance units.

The mobilities of the metal-NTA complexes were consistently lower than those of the corresponding metal-EDTA complexes, indicating that they traveled more slowly through the electrolyte. This was to be expected since, although smaller in size, the metal-NTA complexes also possess a smaller charge than the metal-EDTA complexes and therefore a smaller charge density. Cadmium and Pb were not detected as NTA complexes at 185 nm.

Separation of Mixed Metal Complexes by CE. The electropherogram in Figure 4 illustrates the simultaneous separation of three metal-NTA complexes from the parent NTA moiety. Baseline resolution occurred in less than 5 min. The order of elution was NTA < CuNTA < ZnNTA < NiNTA. The concentrations determined using CE closely agreed with those predicted by GEOCHEM. CoNTA eluted at a similar time to ZnNTA and for simplicity is not shown.

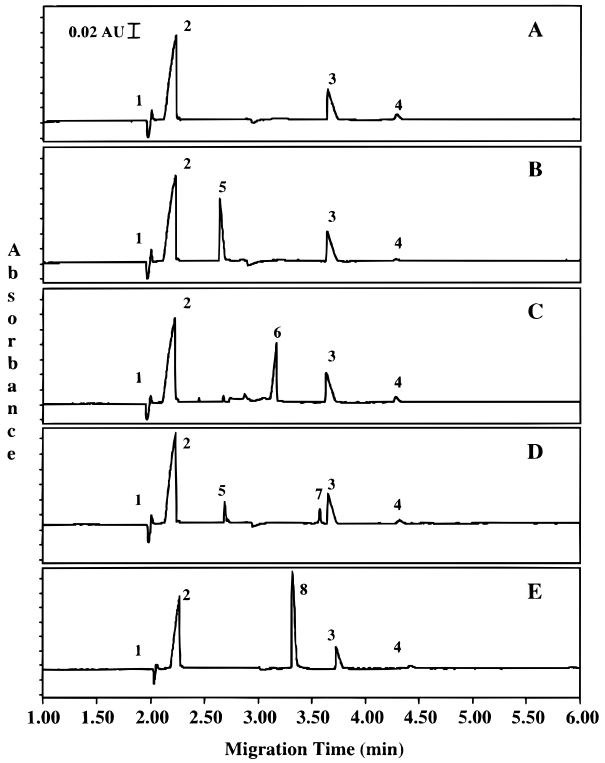

FIGURE 5. Electropherograms of nutrient solutions containing either no added ligand (A), 2 mM NTA (B), 2 mM EDTA (C), 500 μM NTA + 250 μM $ZnSO_4$ (D), or 2 mM FeNaEDTA (E). Peak identity: (1) Cl, (2) NO_3, (3) MES, (4) FeHBED, (5) NTA, (6) CaEDTA, (7) ZnNTA, (8) FeEDTA. Conditions: 25 mM phosphate buffer and 0.5 mM TTAB (pH 6.86), 185 nm, 20 kV, 25 °C. AU = absorbance units.

It was not possible to separate all of the metal-EDTA complexes under the same conditions. This probably occurs because of the metal-encapsulated nature of the EDTA complexes, so that the hydrodynamic volume of the different complexes is not substantially different for any given cation. An alternative reason is the broadening of the complex peak resulting from adsorption of the complex to the capillary wall. Separation of these complex species could possibly be achieved using a longer capillary. Baraj et al. (*27*) reported the on-column resolution of CuEDTA and PbEDTA in a 0.1 M acetate buffer upon doubling the total length of the capillary from 46.5 to 80 cm. Increased resolution could also be obtained using capillaries with a smaller internal diameter or increasing the pH of the buffer. The coupling of the CE with other detectors such as MS should be considered given the recent success of Baron and Hering (*12*) in using ES/MS to identify free and metal complexes of EDTA. However, none of these options were investigated because our primary concern was initially to distinguish between free and complexed ligand.

CE of Nutrient Solution. A typical full nutrient solution (*21*), despite containing a complex mix of inorganic salts, resulted in only four significant peaks in phosphate buffer at 185 nm (Figure 5A). The largest peak corresponds to the nitrate anion, the major constituent of the nutrient solution, preceded by a much smaller peak corresponding to the chloride anion. The final two peaks correspond to MES and FeHBED; therefore, CE also provides a useful technique to monitor the concentration of these species in solution. HBED is an aminocarboxylic acid having such a high affinity for Fe [log K = 42.30 (*25*)] and present in only a relatively small amount that the possibility of competitive complexation of Fe(III) in the nutrient solution by either NTA or EDTA can safely be ignored.

The inclusion of 2 mM NTA to the nutrient solution results in the appearance of a single peak corresponding to free NTA near 2.64 min (Figure 5B). There was no reduction in peak corrected area when compared to a NTA solution of equivalent concentration prepared in water. This indicated that NTA remained largely uncomplexed by cations present in the nutrient solution or that the complexes formed in such low concentrations that they were below the detection limits of this method. Speciation calculations for 2 mM NTA indicate that 64.3% should be complexed as CaNTA, 31.1% as free NTA, 4.0% as MgNTA, and 0.5% as MnNTA. This disagreed with the observed electropherogram, which showed no significant decrease in the NTA peak. This indicated that any of the metal complexes formed with NTA were not stable under the separation conditions or in the case of Mg or Mn were below the detection limits of this method. No peaks corresponding to a metal complex were observed for either PbNTA or CdNTA, even though speciation calculations indicate near 100% complex formation. Like Ca, these metals have large ionic radii that result in a low-charge density for the cation and contribute to the instability of the overall complex in the applied electric field.

In contrast, nutrient solution containing 2 mM EDTA run under identical conditions results in several small peaks of poor shape with a single well-defined peak near 3.16 min (Figure 5C). This peak corresponds to a species having a much lower mobility than free EDTA, which elutes slightly after free NTA in aqueous solution. Given the major cation composition of the nutrient solution (3.55 mM Ca and 1.45 mM Mg), the most likely candidate for this compound is CaEDTA. Fukushi et al. (*13*) used 2 mM EDTA in 20 mM sodium tetraborate buffer at pH 9.2 to resolve CaEDTA and MgEDTA, showing that CaEDTA eluted first and had a larger absorbance than MgEDTA. Speciation calculations for 2 mM EDTA indicated that 98.3% should be complexed as CaEDTA, 1.2% as MgEDTA, and 0.5% as MnEDTA. This tends to support the assignment of this peak to Ca rather than Mg.

In the presence of added metal, the equilibrium rapidly shifts to the formation of the transition metal complex due to these compounds significantly greater stability, and the peak corresponding to the Ca complex completely disappears (Figure 5D,E). In the presence of excess NTA (500 μM) over Zn (250 μM), two peaks corresponding to free NTA and ZnNTA are observed (Figure 5D). GEOCHEM calculations predict NTA to speciate as ZnNTA (50.1%), CaNTA (35.7%), and free NTA (11.3%). However, as noted above, the species CaNTA is unstable and, therefore, not observed in this buffer system. Excluding CaNTA formation from the calculations gives only two main species: ZnNTA (50.2%) and NTA (42.1%). This agrees closely with the determined speciation using CE: ZnNTA (50%) and NTA (44%).

Nutrient solution containing 2 mM FeNaEDTA results in a single additional peak corresponding to the FeEDTA complex (Figure 5E). Speciation calculations for this solution predict that 99.9% of the EDTA should be complexed with Fe(III), which is in good agreement with the speciation determined using CE (91.5%).

In conclusion, the utility of capillary electrophoretic methods for the study of speciation of EDTA and NTA with a range of metals in aqueous solution and nutrient media has been demonstrated. Samples required no complex pretreatment prior to analysis, and baseline resolution of most peaks of interest was obtained in less than 6 min. The proposed method is suitable for speciation studies involving the majority of transition metals but is poorly suited to the speciation of Ca, Pb, and Cd with NTA due to the kinetic instability of the complexes. Likewise, speciation of CaEDTA or CoNTA is problematic in this buffer system due to ligand exchange with the buffer. Future work planned for this

laboratory is adapting this simple method to soil solutions and xylem sap exudate.

Acknowledgments

The authors gratefully acknowledge the financial support provided by the University of Adelaide Research Scheme.

Literature Cited

(1) Huang, J. W.; Chen, J.; Berti, W. R.; Cunningham, S. D. *Environ. Sci. Technol.* **1997**, *31* (3), 800−805.
(2) Blaylock, M. J.; Salt, D. E.; Dushenkov, S.; Zakharova, O.; Gussman, C.; Kapulnik, Y.; Ensley, B. D.; Raskin, I. *Environ. Sci. Technol.* **1997**, *31* (3), 860−865.
(3) Vassil, A. D.; Kapulnik, Y.; Raskin, I.; Salt, D. E. *Plant Physiol.* **1998**, *117*, 447−453.
(4) Parker, D. R.; Chaney, R. L.; Norvell, W. A. In *Chemical Equilibrium and Reaction Models*; Loeppert, R. H., Schwab, A. P., Goldberg, S., Eds.; Soil Science Society of America: Madison, WI, 1995; pp 163−200.
(5) Nowack, B.; Kari, F. G.; Hilger, S. U.; Sigg, L. *Anal. Chem*. **1996**, *68* (3), 561−566.
(6) Kari, F. G.; Giger, W. *Water Res.* **1996**, *30* (1), 122−134.
(7) Taylor, D. L.; Jardine, P. M. *J. Environ. Qual.* **1995**, *24* (4), 789−792.
(8) Sheppard, R. L.; Henion, J. *Anal. Chem*. **1997**, *69* (15), 2901−2907.
(9) Blatny, P.; Kvasnicka, F.; Kenndler, E. *J. Chromatogr. A* **1997**, *757*, 297−302.
(10) Kvasnicka, F.; Mikova, K. *J. Food Compos. Anal.* **1996**, *9* (3), 231−242.
(11) Haumann, I.; Bächmann, K. *J. Chromatogr. A* **1995**, *717*, 385−391.
(12) Baron, D.; Hering, J. G. *J. Environ. Qual.* **1998**, *27* (4), 844−850.
(13) Fukushi, K.; Takeda, S.; Wakida, S.; Higashi, K.; Hiiro, K. *J. Chromatogr. A* **1997**, *759*, 211−216.
(14) Conradi, S.; Vogt, C.; Wittrisch, H.; Knobloch, G.; Werner, G. *J. Chromatogr. A* **1996**, *745*, 103−109.
(15) Harvey, S. D. *J. Chromatogr. A* **1996**, *736*, 333−340.
(16) Semenova, O. P.; Timerbaev, A. R.; Gagstädter, R.; Bonn, G. K. *J. High Resolut. Chromatogr.* **1996**, *19*, 177−179.
(17) Liu, W.; Lee, H. K. *J. Chromatogr. A* **1998**, *796*, 385−395.
(18) Jung, G. Y.; Kim, Y. S.; Lim, H. B. *Anal. Sci.* **1997**, *13* (3), 463−467.
(19) Schäffer, S.; Gareil, P.; Carpot, L.; Dezael, C. *J. Chromatogr. A* **1995**, *717*, 351−362.
(20) Bürgisser, C. S.; Stone, A. T. *Environ. Sci. Technol.* **1997**, *31* (9), 2656−2664.
(21) Smolders, E.; McLaughlin, M. J. *Plant Soil* **1996**, *179*, 57−64.
(22) Weast, R. C., Ed. *Handbook of Chemistry and Physics*, 50th ed.; Chemical Rubber Company: Cleveland, OH, 1970; D-101.
(23) Padarauskas, A.; Schwedt, G. *J. Chromatogr. A* **1997**, *773*, 351−360.
(24) Issaq, H. J.; Janini, G. M.; Chan, K. C.; El Rassi, Z. In *Advances in Chromatography*, Vol. 35; Grushka, G., Brown, P. R., Eds.; Marcel Dekker: New York, 1995; pp 101−169.
(25) Parker, D. R.; Norvell, W. A.; Chaney, R. L. In *Chemical Equilibrium and Reaction Models*; Loeppert, R. H., Schwab, A. P., Goldberg, S., Eds.; Soil Science Society of America: Madison, WI, 1995; pp 253−269.
(26) Atkins, P. W. *Physical Chemistry*, 3rd ed.; Oxford University Press: Oxford, 1986; p 669.
(27) Baraj, B.; Martinez, M.; Sastre, A.; Aguilar, M. *J. Chromatogr. A* **1995**, *695*, 103−111.

Received for review March 19, 1999. Revised manuscript received September 30, 1999. Accepted November 11, 1999.

ES990309M